Biochemical and Biophysical Research Communications 456 (2015) 489–493

Contents lists available at ScienceDirect

Biochemical and Biophysical Research Communications

journal homepage: www.elsevier.com/locate/ybbrc

Evidence for the existence of FGFR1–5-HT1A heteroreceptor complexes in the midbrain raphe 5-HT system

Dasiel O. Borroto-Escuela [a], Manuel Narvaez [b], Mileidys Pérez-Alea [c], Alexander O. Tarakanov [d], Antonio Jiménez-Beristain [a], Giuseppa Mudó [e], Luigi F. Agnati [a], Francisco Ciruela [f], Natale Belluardo [e], Kjell Fuxe [a,*]

[a] Department of Neuroscience, Karolinska Institutet, Stockholm, Sweden
[b] Department of Physiology, School of Medicine, University of Málaga, Spain
[c] Lab Animal Models and Cancer Laboratory Anatomy Pathology Program, Institut de Recerca Vall d'Hebron, 08035 Barcelona, Spain
[d] Russian Academy of Sciences, St. Petersburg Institute for Informatics and Automation, Saint Petersburg, Russia
[e] Department of Experimental Biomedicine and Clinical Neurosciences, Laboratory of Molecular Neurobiology, University of Palermo, Palermo, Italy
[f] Unitat de Farmacologia, Departament Patologia i Terapèutica Experimental, Universitat de Barcelona, Spain

ARTICLE INFO

Article history:
Received 9 November 2014
Available online 6 December 2014

Keywords:
G-protein-coupled receptors
Receptor tyrosine kinases
Fibroblast growth factor receptor 1
Serotonin receptors
Heteroreceptor complex
Dimerization

ABSTRACT

The ascending midbrain 5-HT neurons known to contain 5-HT1A autoreceptors may be dysregulated in depression due to a reduced trophic support. With *in situ* proximity ligation assay (PLA) and supported by co-location of the FGFR1 and 5-HT1A immunoreactivities in midbrain raphe 5-HT cells, evidence for the existence of FGFR1–5-HT1A heteroreceptor complexes were obtained in the dorsal and median raphe nuclei of the Sprague–Dawley rat. Their existence in the rat medullary raphe RN33B cell cultures was also established. After combined FGF-2 and 8-OH-DPAT treatment, a marked and significant increase in PLA positive clusters was found in the RN33B cells. Similar results were reached upon coactivation by agonists in HEK293T cells using the Fluorescent Resonance Energy Transfer (FRET) technique resulting in increased FRETmax and reduced FRET50 values. The heteroreceptor complex formation was dependent on TMV of the 5-HT1A receptor since it was blocked by incubation with TMV but not with TMII. Taken together, the 5-HT1A autoreceptors by being recruited into a FGFR1–5-HT1A heteroreceptor complex in the midbrain raphe 5-HT nerve cells may develop a novel function, namely a trophic role in many midbrain 5-HT neuron systems originating from the dorsal and medianus raphe nuclei.

1. Introduction

There is evidence for the existence of direct (heteroreceptor complexes) and/or indirect G protein coupled receptor (GPCR)–receptor tyrosine kinase (RTK) interactions [1–5]. Even in the absence of neurotrophic factor binding to the RTK they can lead to transactivation of RTKs and produce effects on cell proliferation, differentiation and neuronal plasticity [6].

We recently presented evidence for the existence of FGFR1–5-HT1A heteroreceptor complexes in the rat hippocampus with a partial characterization of their interface [7]. The findings demonstrated their enhancing role in hippocampal plasticity which was proposed to play a role in reversing the depression-induced atrophy of hippocampal neurons [7].

Evidence is presented in the current work for the existence of FGFR1–5-HT1A heteroreceptor complexes in midbrain raphe 5-HT nerve cells. This demonstration makes it likely that antidepressant drugs by increasing extracellular 5-HT levels in the midbrain raphe nuclei, not only increases 5-HT1A autoreceptor signaling but also produce an enhanced activation of the FGFR1 receptor protomer in this heteroreceptor complex leading to increased trophism of the 5-HT nerve cells. In line with this hypothesis, extended treatment with the selective 5-HT re-uptake inhibitor zimelidine caused increases in 5-HT immunofluorescence in the dorsal raphe cells [8].

* Corresponding author at: Retzius väg 8, 17177 Stockholm, Sweden. Fax: +46 8 315721.
E-mail addresses: Dasiel.Borroto.Escuela@ki.se (D.O. Borroto-Escuela), mnarvaez@uma.es (M. Narvaez), mileidys.perez@vhir.org (M. Pérez-Alea), tar@iias.spb.su (A.O. Tarakanov), Tony.jimenez-beristain@ki.se (A. Jiménez-Beristain), g.mudo@unipa.it (G. Mudó), luigiagnati@tin.it (L.F. Agnati), fciruela@ub.edu (F. Ciruela), n.belluardo@unipa.it (N. Belluardo), Kjell.Fuxe@ki.se (K. Fuxe).

http://dx.doi.org/10.1016/j.bbrc.2014.11.112
0006-291X/

2. Materials and methods

2.1. Plasmid constructs

The cDNA encoding the human 5-HT1A and FGFR1 without its stop codon was subcloned in $pGFP^2$-N1 (Perkin-Elmer, Madrid, Spain) and pEYFP-N1 (Clontech, Heidelberg, Germany) using standard molecular biology and PCR techniques [9,10].

2.2. Cell culture and transfection

HEK293T or RN33B cells (a CNS-derived neuronal precursor cell line [11]) (American Type Culture Collection, Manassas, VA, USA) were grown in Dulbecco's modified Eagle's medium/F12 supplemented with 2 mM L-glutamine, 100 units/ml penicillin/streptomycin, and 10% (v/v) foetal bovine serum (FBS) at 37 °C and in an atmosphere of 5% CO_2. For transfection, cells were plated in 6-well dishes at a concentration of 1×10^6 cells/well or in 75 cm^2 flasks and cultured overnight before transfection. Cells were transiently transfected (cDNA molar ratio 1:1) using linear PolyEthylenImine reagent (PEI) (Polysciences Inc., Warrenton, PA, USA).

2.3. Double immunolabeling histochemistry

Adult age-matched male Sprague–Dawley rats ($n = 3$) were anesthetized and perfused intracardially with 4% (wt/vol) paraformaldehyde in phosphate-buffered saline (PBS). Brains were removed, post-fixed by immersion overnight in 4% paraformaldehyde in PBS and coronal sections (20 μm) were cut on a vibratome and processed for free-floating immunohistochemistry. Sections were permeabilized with buffer A containing 0.2% Triton X-100 for 5 min, and then preincubated in a blocking buffer containing 0.3% (wt/vol) triton and 4% (wt/vol) bovine serum albumin. After 1 h at room temperature, sections were labeled with the indicated primary antibodies for 1 h, extensively washed, and stained with the indicated fluorescence labeled secondary antibodies. Samples were rinsed and visualized employing a Leica SP2 confocal microscope. The primary antibodies used were as follows: rabbit polyclonal antiserum against 5-HT1A receptor (ab44635) (5 μg/ml; Abcam, Stockholm, Sweden) and mouse monoclonal [M2F12] (ab829) antibodies against FGFR1 (5 μg/ml; Abcam, Stockholm, Sweden). The secondary antibodies used were as follows: Alexa Fluor 488-conjugated goat anti-mouse IgG (1:2000; Invitrogen, Stockholm, Sweden), Alexa Fluor 546-conjugated goat anti-rabbit IgG (1:2000; Invitrogen, Stockholm, Sweden).

2.4. In situ proximity ligation assay

In situ proximity ligation assay (in situ PLA) was performed as described previously [12]. Free-floating formalin fixed brain sections ($n = 3$, male Sprague–Dawley rats) and RN33B cell cultures were employed using the following primary antibodies: rabbit monoclonal anti-5HT1A (VTG Biosciences) and mouse monoclonal anti-FGFR1 (Abcam). Control experiments employed only one primary antibody or cells transfected with cDNAs encoding only one type of receptor. The PLA signal was visualized and quantified by using a confocal microscope Leica TCS-SL confocal microscope (Leica, USA) and the Duolink Image Tool software.

2.5. Transmembrane peptide treatment

A series of peptides, representing each of the predicted TM segments for the human 5-HT1A (UniProt identifier number: P08908) were synthesized by VTG Biosciences (Stockholm, Sweden) by using 9-fluorenylmethoxycarbonyl chemistry and purified by means of high-performance liquid chromatography (HPLC) analysis (reverse phase C4 column) to ⩾98% purity. TM-I peptide consisted of residues 37–62 (VITSLLLGTLIFCAVLGNACVVAAIA); TM-II peptide of residues 74–98 (LIGSLAVTDLMVSVLVLPMAALYQV); TM-III peptide of residues 110–132 (DLFIALDVLCCTSSILHLCAIAL); TM-IV peptide of residues 153–178 (AAALISLTWLIGFLISIPP MLGWRTP); TM-V peptide of residues 192–217 (DHGYTIYST FGAFYIPLLLMLVLYGR); TM-VI peptide of residues 346–367 (TLGIIMGTFILCWLPFFIVALV); and TM-VII peptide of residues 379–403 (TLLGAIINWLGYSNSLLNPVIYAYF). At the C-terminal juxtamembrane sequence of each TM peptide was introduced the tribasic sequence (RKR) as found in many membrane proteins in order to reduce possible artifact formation through disulfide bridges and to ensure incorporation into the plasma membrane of cells as demonstrated previously [7]. Immediately before use, the peptides were solubilized in dimethyl sulfoxide (DMSO) and diluted in the corresponding cell culture medium to yield a final concentration of 1% DMSO. We verified that, for each tested concentration of DMSO alone, no effect on cell viability was observed. Cells were incubated with the above mentioned peptides at 37 °C for 2 h prior to performing FRET analysis or *in situ* PLA assays. Incorporation of the peptide into cellular membranes under these conditions was checked with a rhodamine-labeled TM-I peptide.

2.6. FRET experiments

Forty-eight hours after transfection HEK293T cells with constant (1 μg) or increasing amounts of cDNA of $FGFR1^{GFP2}$ and $5\text{-}HT1A^{YFP}$ or $5\text{-}HT2A^{YFP}$ respectively were rapidly washed twice in PBS, detached, and resuspended in the same buffer. Cell suspensions (40 μg of total protein) were distributed in duplicates into 96-well microplates and GFP^2 and YFP fluorescence were measured with a POLARstar Optima plate reader (BMG Labtech, Offenburg, Germany), using excitation filters at 410 nm (10-nm bandwidth) and 485 nm (12-nm bandwidth), as well as emission filters corresponding to 510 nm (10-nm bandwidth), and 530 nm (10-nm bandwidth), respectively. Mock-transfected cells were used for background subtraction. FRET signals were collected using 410/10 nm excitation and 530/10 nm emission filters. Removal of acceptor bleed-through, the correction of acceptor fluorescence intensity changes and the calculations of the normalized FRET values (n-FRET) were carried out as previously described [13].

2.7. Data analysis

The number of samples (n) in each experimental condition is indicated in figure legends. All data were analyzed using the commercial program GraphPad PRISM 4.0 (GraphPad Software, USA). When two experimental conditions were compared, statistical analysis was performed using an unpaired t test. Otherwise, statistical analysis was performed by one-way analysis of variance (ANOVA) followed by Tukey's Multiple Comparison post-test. The P value 0.05 and lower was considered significant. $^{*}P < 0.05$, $^{**}P < 0.01$, $^{***}P < 0.001$. FRET isotherms were fitted using a nonlinear regression equation assuming a single binding site, which provided FRETmax and FRET50 values.

3. Results

3.1. Existence of FGFR1–5-HT1A heteroreceptor complexes in the dorsal and median raphe nuclei, in raphe RN33B cells and in HEK293T cells

We used three different approaches, *in situ* PLA, FRET technology, supplemented with double immunolabeling procedures.

3.2. Midbrain raphe region

In situ PLA: PLA positive red clusters were found in large number of nerve cells of the dorsal and median raphe nuclei, but were absent elsewhere in the surrounding areas e.g. in the deep gray layer of the superior colliculus and the periaqueductal gray, dorsomedial region (see Fig. 1A and B). Quantitative analysis shows a significant higher number of positive PLA clusters/blobs per sample field (objective 63×, scan field at zoom 1: 238 × 238 μm) in dorsal (128 ± 10) and median raphe (109 ± 11) nuclei compared to control experiments (2.2 ± 0.8) (Fig. 1C). Control experiments employed only one primary anti-body of one of the receptor protomers. The specificity was also demonstrated by the fact that no PLA clusters were observed in HEK293T cells singly transfected with FGFR1 or with the 5-HT1A receptors (Supplementary Fig. S1). Extensive co-localization of FGFR1 and 5-HT1A immunoreactivities was observed in the nerve cells of the dorsal raphe (Supplementary Fig. S2) and the median raphe.

3.3. Raphe RN33B cells

In situ PLA: The existence of FGFR1–5-HT1A heteroreceptor complexes was also demonstrated with PLA in raphe RN33B cells. The mean number of PLA positive red clusters/blobs per cell was found to be significantly increased by FGF-2 or 8-OH-DPAT treatment alone. This increase was significantly and markedly enhanced by combined treatment (Fig. 2).

3.4. HEK293T cells

FRET technique: A saturation FRET curve was obtained in HEK293T cells co-expressing a constant amount of the FGFR1-GFP2 plasmid while increasing the amount of the 5-HT1A-YFP plasmid which was not obtained with the 5-HT2A-YFP plasmid. Thus, cotransfection of FGFR1 and 5-HT2A led only to a linear regression and thus these receptors failed to specifically interact (Fig. 3-left). Treatment of 5HT1A–FGFR1 cotransfected cells with the agonist ligands FGF-2 and 8-OH-DPAT significantly reduced the FRET50 values and increased the FRETmax signal (Fig. 3-left). Thus, the combined treatment substantially increased the recruitment of the heteroreceptor complex and the affinity of the interaction between the two protomers. In FRET experiments we observed that the most important TM interface interaction of the FGFR1–5-HT1A heteroreceptor complex involves the TM-V (Fig. 3-right) and potentially also TM-VII (not shown). FRET competition experiments with synthetic peptides of TMII and TMV of the 5-HT1A receptor were performed (Fig. 3-right). TMV incubation resulted in a significant and complete loss of the 5HT1A capacity to interact with FGFR1, while TMII was totally ineffective. Incubation with TM-IV and TM-VI also failed to block the FRET signal (not shown).

4. Discussion

For the first time the existence of FGFR1–5-HT1A heteroreceptor complexes are demonstrated in 5-HT nerve cells of the dorsal and median raphe nuclei of the midbrain by means of the *in situ*

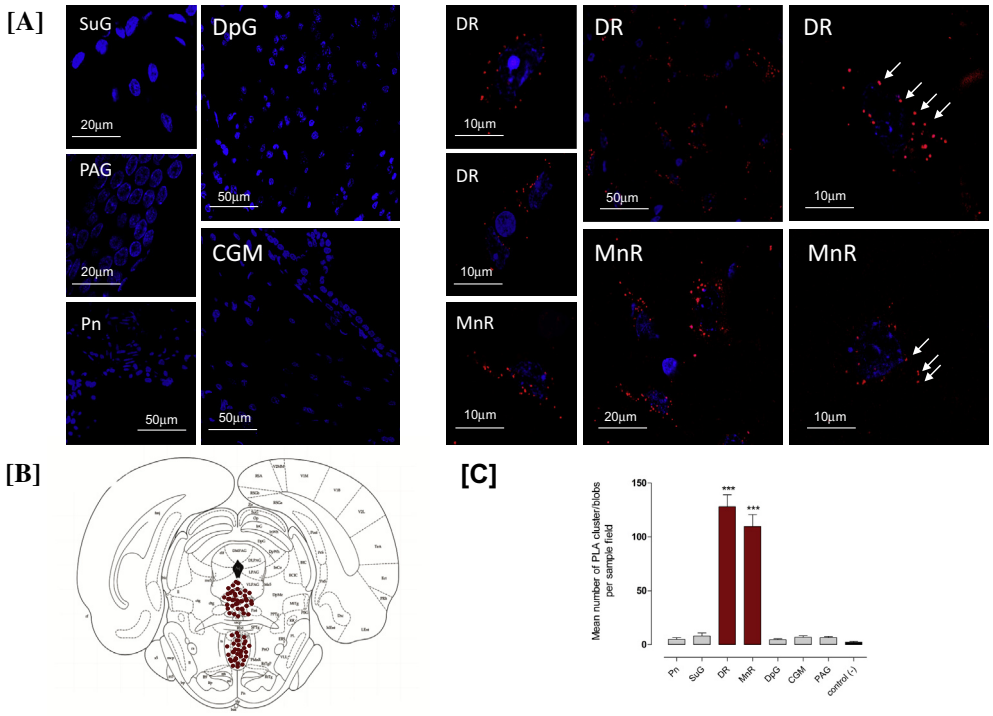

Fig. 1. FGFR1 and 5-HT1A heteroreceptor complexes in midbrain rat sections are detected by *in situ* PLA. (A) Detection of neuronal cytoplasmatic FGFR1–5-HT1A heteroreceptor complexes (seen as red clusters indicated by arrows) in dorsal and median raphe nuclei by *in situ* PLA; nuclei are shown in blue (DAPI). Three independent experiments (three rats) were performed. Bregma level −7.6. MnR: median raphe nucleus; DR: dorsal raphe nucleus, CGM: central gray medial part; DpG: deep gray layer of the superior colliculus; SuG: superficial gray layer of the superior colliculus; PAG: periaqueductal gray, dorsomedial part; Pn: pontine nuclei. (B) The relative densities of PLA cluster distributions within areas of the dorsal and median raphe nucleus are schematically illustrated by the density of red puncta, Bregma level −7.6. (C) Quantitation involves determination of the number of PLA clusters/blobs per sample field in each studied area. Values are represented as a means ± S.E.M. number of PLA clusters/blobs per sample field (objective 63×, scan field at zoom 1: 238 × 238 μm), $n = 3$, 10 replicates. Statistical analysis was performed by one-way analysis of variance (ANOVA) followed by Tukey's Multiple Comparison post-test. DR and MnR groups are significantly different compared to Pn, SuG, DpG, CGM, PAG, control (−) groups (***$P < 0.001$), In negative control experiments only anti-FGFR1 primary antibody was employed followed by the PLA probe positively and negatively tagged secondary antibodies. (For interpretation of the references to color in this figure legend, the reader is referred to the web version of this article.)

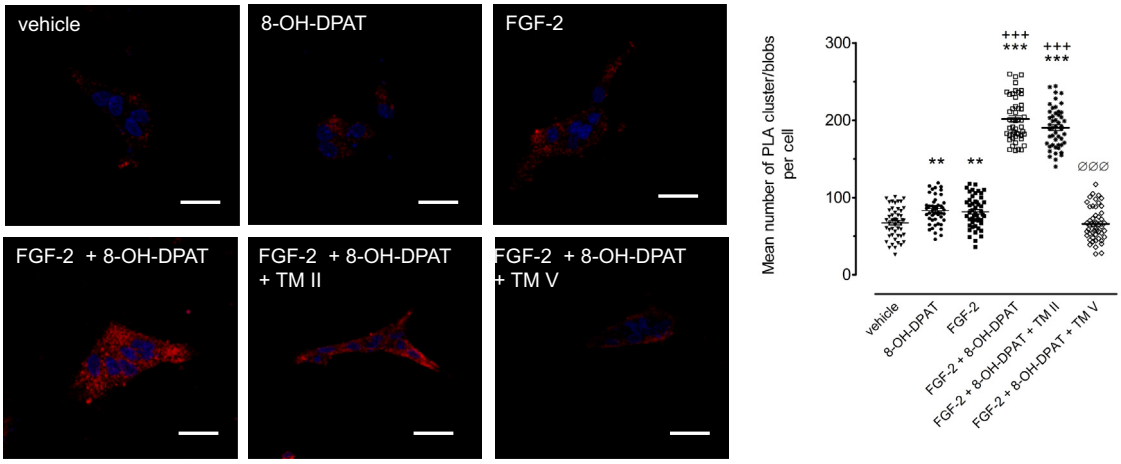

Fig. 2. FGFR1 and 5-HT1A heteroreceptor complexes and their agonist modulation in rat RN33B cells. (left panels) Increased FGFR1–5-HT1A heteroreceptor complex formation was observed upon receptor coactivation in rat raphe RN33B cells. Cells were treated with vehicle (−), 8-OH-DPAT (100 nM), FGF-2 (50 ng/ml) or combined incubation with 8-OH-DPAT + FGF-2 (100 nM and 50 ng/ml, respectively) and the TM peptides (TMII or TMV) (0.4 μM) for 24 h and samples were processed for detection of *in situ* PLA signals. Scale bar = 75 μm. (right panel) Quantification of receptor complexes was performed and expressed as red PLA clusters/blobs per DAPI-positive nuclei in the sample field, giving a value of PLA clusters/blobs per cell, was made in Twelve cells per plate and performed on four plates. Thus each point in the scattered plot represent one cell and all the cells (48 cells) from the four different experiments are included. The lines in each group represents the mean value. Statistical analysis was performed ($n = 4$) by one-way analysis of variance (ANOVA) followed by Tukey's Multiple Comparison post-test. 8-OH-DPAT (100 nM) and FGF-2 (50 ng/ml) groups are significantly different compared to vehicle ($^{**}P < 0.01$), combined 8-OH-DPAT + FGF-2 and 8-OH-DPAT + FGF-2 + TMII groups are significantly different compared to 8-OH-DPAT (100 nM) and FGF-2 (50 ng/ml) alone group ($^{+++}P < 0.001$) or vehicle group (***: $P < 0.001$). 8-OH-DPAT + FGF-2 + TMV group is significantly different compared to combined 8-OH-DPAT + FGF-2 and 8-OH-DPAT + FGF-2 + TMII groups (000: $P < 0.001$). The mean cluster per cells in the negative controls (cells only incubated with the primary anti-FGFR1 antibody) is 6.0 ± 1.0, a total of 48 cells from four different experiments (12 cells per experiments) are included.

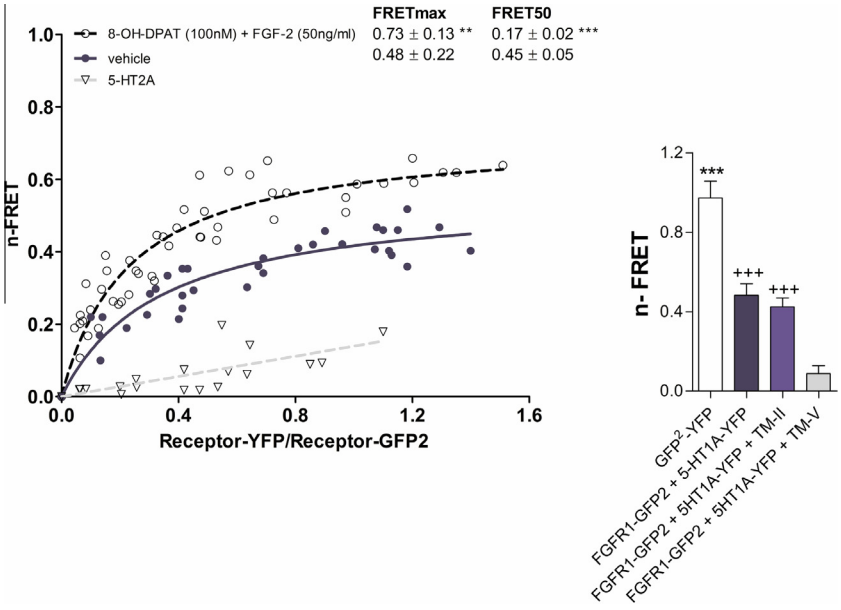

Fig. 3. FRET shows specific 5-HT1A and FGFR1 heteromerization in HEK293T cells. (left panel) FRET saturation curves were generated in HEK293T cells expressing a fixed amount of FGFR1-GFP2 and increasing amounts of 5-HT1A-YFP or 5HT2A-YFP. Cells were pre-incubated 10 min with vehicle or with 8-OH-DPAT and FGF-2 (100 nM and 50 ng/ml). The FRETmax values were significantly increased by combined 8-OH-DPAT and FGF-2 treatment versus vehicle ($^{**}P < 0.01$); and the FRET50 value of the combined treatment group was significantly reduced versus vehicle group ($^{***}P < 0.001$). The 5-HT1A/FGFR1 curve fitted better to a saturation curve than to a linear regression as found with 5HT2A/FGFR1 (F test ($P < 0.001$). Data are means ± S.E.M. ($n = 5$). (right panel) The effects of different 5-HT1A receptor TM synthetic peptides are shown on FRET signals of the 5-HT1A–FGFR1 heteroreceptor complexes. Values represent the maximal saturable normalized FRET values. Means ± S.E.M.; $n = 4$, 6 replicates. Statistical analysis was performed by one-way analysis of variance (ANOVA) followed by Tukey's Multiple Comparison post-test. The (FGFR1-GFP2 + 5HT1A-YFP) and (FGFR1-GFP2 + 5HT1A-YFP + TM peptide II) groups as well as the chimera group (GFP2-YFP; positive control) are significantly different from the (FGFR1-GFP2 + 5HT1A-YFP + TM peptide V) group ($^{+++}P < 0.001$ and $^{***}P < 0.001$ respectively). The concentration of the synthetic TM peptides used is 0.4 μM in all experiments.

PLA technique as previously postulated [4]. These 5-HT neurons are known from previous work to express FGFR1 and to contain high amounts of 5-HT1A immunoreactivity and a high density of 5-HT1A binding sites [14–16]. The PLA positive clusters have a location in the cytoplasm and are also associated with the plasma membrane. They were in addition demonstrated in the current study with the *in situ* PLA technique in stable cell lines from the medullary raphe neurons, known to contain 5-HT IR in their cytoplasm [17]. The specificity of the *in situ* PLA assay was indicated from the almost complete absence of the PLA clusters in HEK293T cells singly transfected with FGFR1 or 5-HT1A. Further specificity is given from the very low density of PLA positive clusters in negative

controls (only one primary antibody used) from the raphe nuclei and the selective location of the PLA positive clusters in the midbrain raphe nuclei. Also co-location of FGFR1 and 5-HT1A immunoreactivities was demonstrated in the majority of the 5-HT nerve cells within the dorsal and median raphe nuclei in line with the presence of FGFR1 mRNA levels in the midbrain 5-HT nerve cells [14].

With the FRET technique the existence of the FGFR1–5-HT1A heteroreceptor complexes were also demonstrated in HEK293T cells transiently cotransfected with FGFR1-GFP2 and 5-HT1A-YFP. The FRET results also indicated that combined treatment with FGF-2 and 8-OH-DPAT may recruit an increased number of FGFR1–5-HT1A heteroreceptor complexes with an increased affinity of their interaction in view of the increased FRETmax and reduced FRET50 values observed with this combined agonist treatment. In line with this interpretation the number of PLA positive clusters per nerve cell markedly increased upon this cotreatment. This increase was blocked by incubation with the TMV peptide but not the TMII peptide of the 5-HT1A receptor indicating that TMV is part of the receptor interface.

These results open up the possibility that the 5-HT1A autoreceptors may also participate in the neurotrophism of the central 5-HT nerve cells via the formation of FGFR1–5-HT1A heteroreceptor complexes which may be dynamically regulated by combined agonist treatment. The 5-HT1A autoreceptors by being part of a FGFR1–5-HT1A heteroreceptor complex in the midbrain raphe 5-HT nerve cells appears to have an additional functional role in midbrain 5-HT neuron systems besides playing a key role in reducing the activity of these neurons by acting as an autoreceptor [15,18]. Thus, by transactivation of FGFR1 in this heteroreceptor complex and increasing its ERK1/2 signaling it may improve the neuroplasticity of the 5-HT nerve cells which can contribute to antidepressant like effects. At the same time the 5-HT1A autoreceptor may become uncoupled from the GIRK channels of the 5-HT nerve cells as it is recruited to the 5-HT1A-FGFR1 heteroreceptor complex upon agonist coactivation. This change of function likely reduces its inhibitory actions on the firing of the midbrain 5-HT neurons expressing these receptor complexes and also likely contributes to antidepressant actions.

It may be speculated that certain types of depression may develop as a result of a disruption of the FGFR1–5-HT1A heteroreceptor complex in midbrain 5-HT raphe cells and their hippocampal target neurons [13]. This reduces the neuroplasticity and trophism of the central 5-HT neurons and leads to dysregulation of the 5-HT1A autoreceptor with abnormal reductions of the firing rate in these neurons. Such events would have consequences for the parts of the tel-and diencephalon innervated and modulated by the large number of ascending 5-HT neurons containing the FGFR1–5-HT1A heteroreceptor complexes. They form global 5-HT nerve terminal networks operating via extrasynaptic volume transmission [19]. Future work will show if this hypothesis has a value in understanding mechanisms of major depression and its treatment.

Acknowledgments

This work has been supported by the Swedish Royal Academy of Sciences (KWA) and Karolinska Institutets Forskningsstiftelser 2011 and 2012 to D.O.B-E, by grants from the Swedish Medical Research Council (04X-715), Telethon TV3's La Marató Foundation 2008, Torsten and Ragnar Söderberg Foundation and Hjärnfonden to K.F. Wilber Romero-Fernández is acknowledged for his help in the immunohistochemistry experiments. A.O.T. has not received any support for this work.

Appendix A. Supplementary data

Supplementary data associated with this article can be found, in the online version, at http://dx.doi.org/10.1016/j.bbrc.2014.11.112.

References

[1] L.M. Luttrell, Y. Daaka, R.J. Lefkowitz, Regulation of tyrosine kinase Cascades by G-protein-coupled receptors, Curr. Opin. Cell Biol. 11 (1999) 177–183.
[2] F.S. Lee, R. Rajagopal, M.V. Chao, Distinctive features of Trk neurotrophin receptor transactivation by G protein-coupled receptors, Cytokine Growth Factor Rev. 13 (2002) 11–17.
[3] B.H. Shah, K.J. Catt, GPCR-mediated transactivation of RTKs in the CNS: mechanisms and consequences, Trends Neurosci. 27 (2004) 48–53.
[4] K. Fuxe, A. Dahlstrom, M. Hoistad, D. Marcellino, A. Jansson, A. Rivera, Z. Diaz-Cabiale, K. Jacobsen, B. Tinner-Staines, B. Hagman, G. Leo, W. Staines, D. Guidolin, J. Kehr, S. Genedani, N. Belluardo, L.F. Agnati, From the Golgi–Cajal mapping to the transmitter-based characterization of the neuronal networks leading to two modes of brain communication: wiring and volume transmission, Brain Res. Rev. 55 (2007) 17–54.
[5] E. Castren, V. Voikar, T. Rantamaki, Role of neurotrophic factors in depression, Curr. Opin. Pharmacol. 7 (2007) 18–21.
[6] F.S. Lee, M.V. Chao, Activation of Trk neurotrophin receptors in the absence of neurotrophins, Proc. Natl. Acad. Sci. U.S.A. 98 (2001) 3555–3560.
[7] D.O. Borroto-Escuela, W. Romero-Fernandez, G. Mudo, M. Perez-Alea, F. Ciruela, A.O. Tarakanov, M. Narvaez, V. Di Liberto, L.F. Agnati, N. Belluardo, K. Fuxe, Fibroblast growth factor receptor 1–5-hydroxytryptamine 1A heteroreceptor complexes and their enhancement of hippocampal plasticity, Biol. Psychiatry 71 (2012) 84–91.
[8] K. Fuxe, L.F. Agnati, K. Andersson, L. Calza, F. Benfenati, I. Zini, N. Battistini, C. Kohler, S.O. Ogren, T. Hökfelt, Analysis of trasmitter-identified neurons by morphometry and quantitative microfluorimetry. Evaluations of the actions of psychoative drugs, specially sulpiride, in: M. Ackenheil, N. Matussek (Eds.), Special Aspects of Psychopharmacology, Espansion Scientifique Francaise, Paris, 1983, pp. 13–32.
[9] D.O. Borroto-Escuela, F. Corrales, M. Narvaez, J. Oflijan, L.F. Agnati, M. Palkovits, K. Fuxe, Dynamic modulation of FGFR1–5-HT1A heteroreceptor complexes. Agonist treatment enhances participation of FGFR1 and 5-HT1A homodimers and recruitment of β-arrestin2, Biochem. Biophys. Res. Commun. 441 (2013) 387–392.
[10] D.O. Borroto-Escuela, M. Flajolet, L.F. Agnati, P. Greengard, K. Fuxe, Bioluminescence resonance energy transfer methods to study G protein-coupled receptor–receptor tyrosine kinase heteroreceptor complexes, Methods Cell Biol. 117 (2013) 141–164.
[11] C. Lundberg, U. Englund, D. Trono, A. Bjorklund, K. Wictorin, Differentiation of the RN33B cell line into forebrain projection neurons after transplantation into the neonatal rat brain, Exp. Neurol. 175 (2002) 370–387.
[12] D.O. Borroto-Escuela, W. Romero-Fernandez, P. Garriga, F. Ciruela, M. Narvaez, A.O. Tarakanov, M. Palkovits, L.F. Agnati, K. Fuxe, G protein-coupled receptor heterodimerization in the brain, Methods Enzymol. 521 (2013) 281–294.
[13] K. Fuxe, D.O. Borroto-Escuela, D. Marcellino, W. Romero-Fernandez, M. Frankowska, D. Guidolin, M. Filip, L. Ferraro, A.S. Woods, A. Tarakanov, F. Ciruela, L.F. Agnati, S. Tanganelli, GPCR heteromers and their allosteric receptor–receptor interactions, Curr. Med. Chem. 19 (2012) 356–363.
[14] N. Belluardo, G. Wu, G. Mudo, A.C. Hansson, R. Pettersson, K. Fuxe, Comparative localization of fibroblast growth factor receptor-1, -2, and -3 mRNAs in the rat brain: in situ hybridization analysis, J. Comp. Neurol. 379 (1997) 226–246.
[15] P.R. Albert, P. Lembo, J.M. Storring, A. Charest, C. Saucier, The 5-HT1A receptor: signaling desensitization, and gene transcription, Neuropsychopharmacology 14 (1996) 19–25.
[16] M. Hamon, P. Blier, Monoamine neurocircuitry in depression and strategies for new treatments, Prog. Neuropsychopharmacol. Biol. Psychiatry 45 (2013) 54–63.
[17] M. Czesak, A.M. Burns, F.R. Lenicov, P.R. Albert, Characterization of rat rostral raphe primary cultures: multiplex quantification of serotonergic markers, J. Neurosci. Methods 164 (2007) 59–67.
[18] F. Artigas, L. Romero, C. De Montigny, P. Blier, Acceleration of the effect of selected antidepressant drugs in major depression by 5-HT1A antagonists, Trends Neurosci. 19 (1996) 378–383.
[19] K. Fuxe, D.O. Borroto-Escuela, W. Romero-Fernandez, Z. Diaz-Cabiale, A. Rivera, L. Ferraro, S. Tanganelli, A.O. Tarakanov, P. Garriga, J.A. Narvaez, F. Ciruela, M. Guescini, L.F. Agnati, Extrasynaptic neurotransmission in the modulation of brain function. Focus on the striatal neuronal–glial networks, Front. Physiol. 3 (2012) 136.